MAGNETISM

Pulsed Field-Induced Magnetization Switching in Antiferromagnetic Ferrihydrite Nanoparticles

D. A. Balaev[a, b, *], **A. A. Krasikov**[a], **D. A. Velikanov**[a], **S. I. Popkov**[a, b], **N. V. Dubynin**[c],
S. V. Stolyar[a, b, d], **V. P. Ladygina**[d], **and R. N. Yaroslavtsev**[a, b]

[a] Kirensky Institute of Physics, Krasnoyarsk Scientific Center, Siberian Branch, Russian Academy of Sciences,
Krasnoyarsk, 660036 Russia
[b] Siberian Federal University, Krasnoyarsk, 660041 Russia
[c] Moscow State University of Civil Engineering, Moscow, 129337 Russia
[d] Krasnoyarsk Scientific Center, Siberian Branch, Russian Academy of Sciences, Krasnoyarsk, 660036 Russia
*e-mail: dabalaev@iph.krasn.ru
Received March 13, 2018

Abstract—The dynamic magnetization switching of ferrihydrite nanoparticles has been investigated by a pulsed magnetometer technique in maximum fields H_{max} of up to 130 kOe with pulse lengths of 4, 8, and 16 ms. Ferrihydrite exhibits antiferromagnetic ordering and defects cause the uncompensated magnetic moment in nanoparticles; therefore, the behavior typical of magnetic nanoparticles is observed. The dynamic hysteresis loops measured under the above-mentioned conditions show that the use of pulsed fields significantly broadens the temperature region of existence of the magnetic hysteresis and the coercivity can be governed by varying the maximum field and pulse length. This behavior is resulted from the relaxation effects typical of conventional ferro- and ferrimagnetic nanoparticles and the features typical of antiferromagnetic nanoparticles.

1. INTRODUCTION

Nanoparticles of materials characterized by antiferromagnetic (AFM) ordering exhibit the intriguing magnetic properties [1−3]. This is due to the surface effects and defects (AFM ordering violations). The formation of defects on the surface and in the bulk of particles is related to their crystallochemical properties. The defects lead to the occurrence of an uncompensated magnetic moment in AFM nanoparticles, which can attain hundreds of Bohr magnetons. This offers the opportunity of using AFM nanoparticles in various research directions, including medicine [4, 5].

Along with the existence of uncompensated magnetic moment μ_p, there is a number of other interesting peculiarities in the magnetic behavior of AFM nanoparticles. Similar to ferro- and ferrimagnetic nanoparticles, AFM particles exhibit a superparamagnetic (SP) behavior at temperatures above the characteristic blocking temperature T_B. In the temperature range of $T < T_B$, the $M(H)$ magnetization curves are hysteretic. On the one hand, similar to ferro- and ferrimagnetic nanoparticles, the $M(H)$ hysteresis is related to the competition between the Zeeman energy $\mu_p H$ and the magnetic anisotropy energy $K_{eff}V$ (K_{eff} is the effective magnetic anisotropy constant, which includes the surface anisotropy, and V is the particle

volume). On the other hand, the magnetic moment of an AFM particle can be exchange-coupled with the AFM core, which can give rise to an additional anisotropy. This mechanism possibly manifests itself in the shift of the magnetic hysteresis loop of AFM particles after their cooling in external field from a temperature over T_B [6−13]. In addition, it is worth noting that the magnetization curve of an ensemble of AF nanoparticles is, in the first approximation (with disregard of the exchange coupling between μ_p and the AFM core), a superposition of the contributions of the magnetic moments of particles and the characteristic field-linear magnetic response of the antiferromagnetically ordered core [1, 2, 14−21].

In the conventional investigations of the magnetic hysteresis in quasistatic magnetic fields, the external field variation rate dH/dt is usually no higher than $\sim10^2$ Oe/s. However, study of the dynamical magnetization switching with significantly higher dH/dt values can bring new information, since the variation in the parameter dH/dt affects the relaxation processes [22−24]. The ratio between the T_B, V, and K_{eff} values and characteristic measurement (τ_m) and particle relax-

ation (τ_0) times are determined from the Néel−Brown expression

$$T_B = K_{\text{eff}}V / \ln(\tau_m/\tau_0)k_B, \qquad (1)$$

where k_B is the Boltzmann constant. The τ_0 value can lie between $10^{-9}-10^{-12}$ s and the τ_m value in the quasi-static measurements is about 10^1-10^2 s [1]. The increase in the parameter dH/dt during magnetization is analogous to a decrease in the characteristic time τ_m, which results in the effective growth of the SP blocking temperature and the $M(H)$ dependence reversible in the quasistatic measurements can exhibit the hysteresis under the dynamic magnetization switching.

If the field H_R of the onset of reversible behavior of the $M(H)$ dependence, (i.e., at $H \geq H_R$ the hysteresis loop is closed) is fairly weak (e.g., about 10^3 Oe), then the above-mentioned processes can be observed on facilities generating ac magnetic fields of different frequencies. However, if the H_R value is ~10^4 Oe or more, then the processes of dynamic magnetization switching can be investigated on facilities generating pulsed magnetic fields. Antiferromagnetic nanoparticles belong to the class of objects with the high H_R values [13, 17, 25, 26]. The behavior of coercivity H_C can only be examined on magnetometers operating in strong pulsed magnetic fields.

In our previous work [27], we studied the dynamic magnetization switching of ε-Fe_2O_3 nanoparticles in pulsed magnetic fields. The H_R value of these objects is ~50 kOe. Using the dynamic magnetic hysteresis loops, we obtained the coercivity as a function of the external field variation rate dH/dt, which allowed us to establish the role of surface anisotropy in these objects using a theoretical model of ferromagnetic nanoparticles [22, 23]. In our opinion, it is reasonable to extend these dynamic magnetization switching investigations to AFM nanoparticles. The aim of this study was to establish the regularities in the behavior of dynamic magnetic hysteresis (DMH) loops of antiferromagnetically ordered ferrihydrite.

Ferrihydrite is an iron hydroxide with the nominal formula $5Fe_2O_3 \cdot 9H_2O$, which exists in a nanosized form. Due to the surface and bulk defects, particles 3−5 nm in size have an uncompensated magnetic moment of about $150-300\mu_B$ in [6, 14−16, 26, 28−31]. In addition, ferrihydrite is a part of the biological object ferritin contained in living organisms. Pure ferrihydrite can be obtained chemically or by extracting from the products of vital activity of bacteria cultivated under certain conditions (biogenic ferrihydrite).

The investigations were carried out on the ferrihydrite samples of both types.

2. EXPERIMENTAL

2.1. Fabrication and Characterization of the Ferrihydrite Samples

The technique for preparing biogenic ferrihydrite formed by the *Klebsiella oxytoca* bacteria vital activity was described in detail in [31, 32]. Chemical ferrihydrite was obtained by slow adding the NaOH (1 M) alkali solution to the $FeCl_3$ iron chloride solution (0.02 M) upon constant stirring at room temperature until obtaining the neutral pH value [33]. The prepared samples were annealed in air at 170°C for 24 h. These samples are hereinafter referred to as Bio-FH and Chem-FH.

Analysis of the Mössbauer spectra obtained on an MC-1104Em spectrometer ([57]Co(Cr) source) showed that the data for the obtained samples are in good agreement with the results reported in [31−33] and the annealing did not lead to the occurrence of foreign iron oxide phases. According to the transmission electron microscopy data, the average Bio-FH and Chem-FH particle size $\langle d \rangle$ was ~4 and ~5 nm, respectively.

The static magnetization measurements ($M(T)$ dependences) were performed on a SQUID magnetometer [34].

2.2. Measuring the Dynamic Magnetic Hysteresis Loops

The DMH loops were measured using an induction magnetometer in pulsed magnetic fields induced by a standard method of capacitor bank discharging through a solenoid. The possibility of measuring the hysteresis loops was ensured by the periodic operation of a facility generating pulsed magnetic fields. In this case, the external field was increased to H_{max} (in these experiments, up to 130 kOe), then to a negative value somewhat lower than $|H_{\text{max}}|$, and, after that, to zero (via closing a thyristor unit). The pulse length was varied by switching the capacitor banks to different capacitances. The measurements were performed at pulse lengths τ_P (τ_P is the half-period during which the external field changes from $H = 0$ to H_{max} and then to $H = 0$) of 4, 8, and 16 ms, which, together with the change in the maximum field strength H_{max} in the pulse makes it possible to measure the DMH in a wide range of field variation rates dH/dt ~ 10−80 MOe/s. The measurements were performed at a temperature of 77 K. The magnetic field variation rate at the instant of sample magnetization switching was determined from the near-zero dH/dt value using the experimental $H(t)$ dependences.

3. RESULTS AND DISCUSSION

Figure 1 shows temperature dependences of magnetization $M(T)$ for the investigated samples, which were measured under zero-field cooling conditions
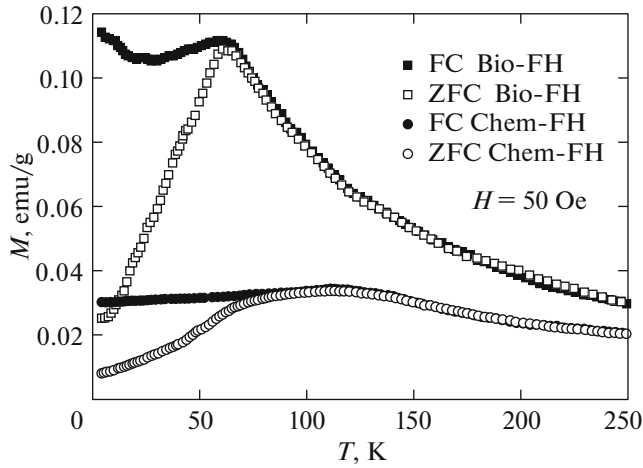
Fig. 1. ZFC and FC temperature dependences of magnetization $M(T)$ for the nanoferrihydrite samples.

(ZFC) and upon cooling in an external field of $H = 50$ Oe (FC). The shape of these dependences shows that the samples under study exhibit a characteristic SP behavior: the pronounced $M(T)_{ZFC}$ maximum and a discrepancy between the $M(T)_{ZFC}$ and $M(T)_{FC}$ dependences. If the SP blocking temperature T_B is determined at the maximum point of the $M(T)_{ZFC}$ dependence, then, the T_B values are 61 and 111 K for the Bio-FH and Chem-FH samples, respectively. At $T \leq T_B$, the discrepancy between the $M(T)_{ZFC}$ and $M(T)_{FC}$ dependences is observed. The T_B values are noticeably higher than those for the initial (unannealed) samples ($\approx$23 and 44 K) and, as was shown previously [31, 35, 36], the increase in the T_B values is related to an increase in the particle size upon low-temperature annealing.

At a temperature of $T = 77$ K, the magnetic moments of Bio-FH particles are in the SP state under the quasistatic magnetic measurement conditions. In these measurements, the $M(H)$ dependences are completely reversible ($H_C = 0$). The T_B value for the Chem-FH sample is somewhat higher than 77 K. However, according to our data, in the quasistatic magnetic measurements (up to 60 kOe), the H_C value at this temperature is no higher than 10^2 Oe.

Figure 2 shows DMH loops for the investigated samples. For the abscissa axis scale used ($\pm$155 kOe), the $M(H)$ data for all the maximum applied field H_{max} values and pulse lengths τ_P lie within the line thickness. The insets in Fig. 2 illustrate the behavior of DMH loops at the origin of coordinates. It can be seen that the $M(H)$ dependences are characterized by the coercivity H_C. The H_C value for DMH loops is determined as an absolute value of the abscissa of the point of intersection of the $M(H)$ dependence with the H axis in the range of $H < 0$. The H_C value depends on the
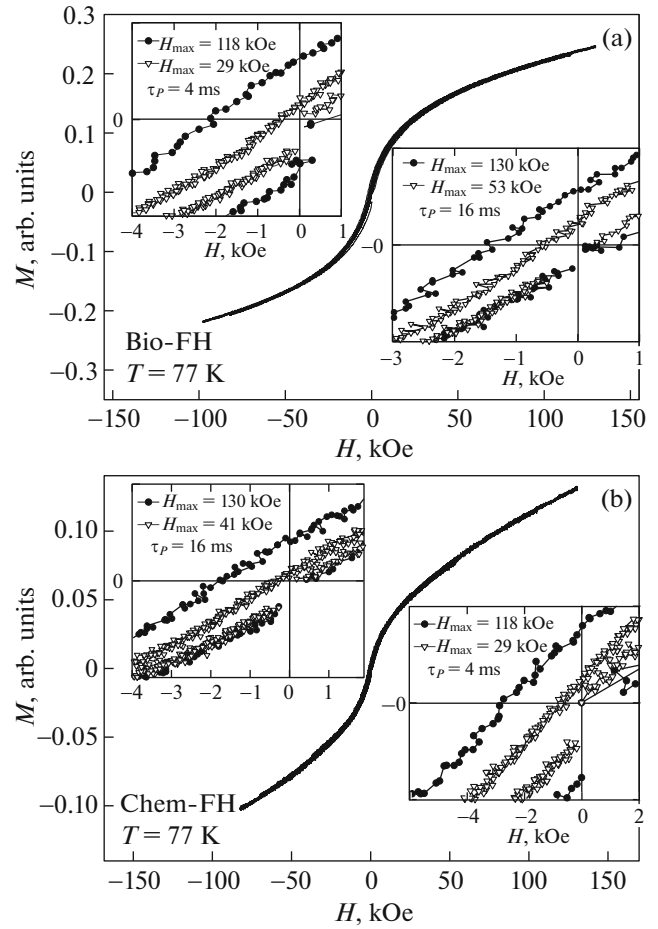

Fig. 2. $M(H)$ dependences under pulsed magnetization switching of (a) biogenic and (b) chemical nanoferrhydrite at $T = 77$ K. Inserts: course of the $M(H)$ dependences at the origin of coordinates at different maximum fields H_{max} and pulse lengths τ_P. Note that under pulsed magnetization switching, the variation in the external field H follows the cycle $0 \rightarrow H_{max} \rightarrow -H_{max} \rightarrow 0$.

pulse length and H_{max} value. The broadening of the region of hysteresis existence under the pulsed magnetization switching can be easily understood by considering the experimental conditions using Eq. (1). Usually, if we speak about the temperature measurements of magnetic susceptibility for the quasistatic measurements, the τ_m value is taken to be 10^1-10^2 s [1]; if we assume τ_m to be the hysteresis loop measurement time, then, at a typical value of $dH/dt \sim 10^1-10^2$ Oe, the τ_m value will be $\sim 10^4$ s. For the case of ac fields with frequency ω, we obviously have $\tau_m = 2\pi/\omega$. If we use this approach in the pulsed measurements, for which $\omega = \pi/\tau_P$ (see Subsection 2.2), then we have $\tau_m = 2\tau_P$. Thus, at the shortest pulse length $\tau_P = 4$ ms, we obtain at $\tau_0 \sim 10^{-10}-10^{-11}$ s that the T_B value increases approximately by a factor of 1.5–1.7 as compared with the quasistatic conditions. This leads to the fact that
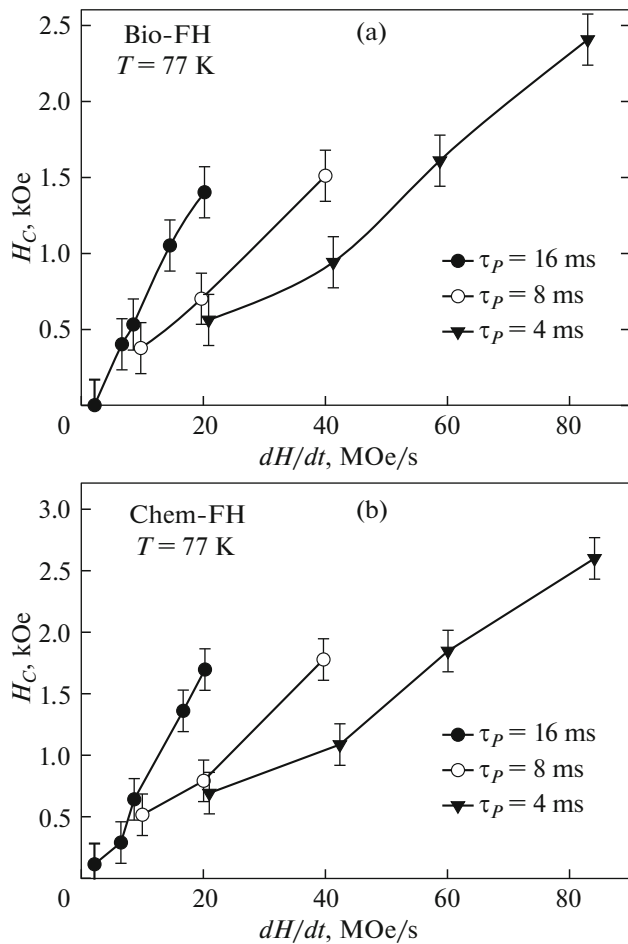
Fig. 3. Dependences of the coercivity H_C under pulsed field-induced magnetization switching as a function of the field variation rate dH/dt for (a) the biogenic and (b) chemical nanoferrihydrite samples at $T = 77$ K. The data are grouped (symbols and lines) by pulse lengths τ_P.

Fig. 4. Dependences of the coercivity H_C under pulsed field-induced magnetization switching as a function of the maximum applied field H_{max} for (a) the biogenic and (b) chemical nanoferrihydrite samples at $T = 77$ K. The data are grouped (symbols and lines) by pulse lengths τ_P.

the effective blocking temperature increases and the measuring temperature 77 K hits the range where the particle magnetic moments are blocked. In principle, the observed coercivity growth with the ac field frequency ($\omega = \pi/\tau_P$) does not contradict the theoretical results for AFM nanoparticles from [24]. However, at this stage of investigations, it is difficult to make a comparison with the theory.

Figure 3 shows the dependence of H_C on the field variation rate dH/dt for the investigated samples. The data in Fig. 3 are grouped (symbols and lines) by pulse lengths τ_P. It can be seen that, despite the general trend of the H_C growth with dH/dt, the bright $H_C(dH/dt)$ dependence is not observed. This behavior differs from the data obtained previously for ε-Fe$_2$O$_3$ nanoparticles [27], which can be considered as single-domain ferro- or ferrimagnetic nanoparticles as applied to the magnetization process [37, 38]. The investigated ferrihydrite samples exhibit AFM order-
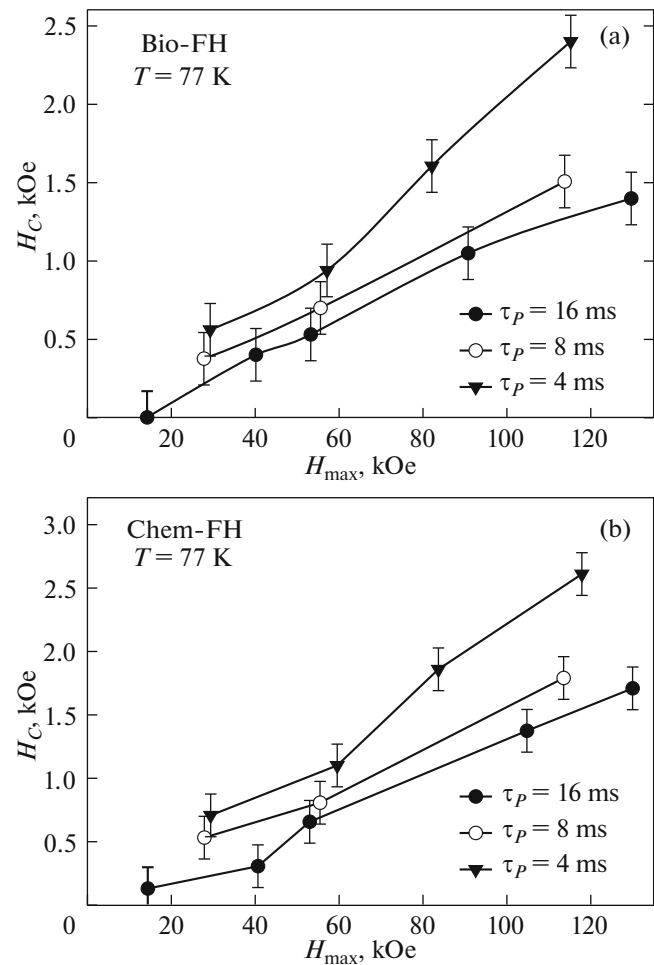
ing; for this kind of particles, there is apparently an additional factor responsible for the coercivity in the DMH measurements. In our opinion, this factor can be the maximum applied field. Indeed, according to the results of investigation of nanoferrihydrites in quasistatic magnetic fields, these objects are characterized by the strong fields of irreversible behavior of magnetization H_R [9, 13], which can attain hundreds of kilooersted at low temperatures. As a result, the H_C value depends on the H_{max} value.

In view of the aforesaid, the coercivity data obtained here are built as a function of the maximum applied field H_{max} (see Fig. 4). Similar to the previous figure, the data are grouped (symbols and connecting lines) by pulse lengths τ_P. It can be seen that the $H_C(H_{max})$ dependences at $\tau_P =$ const are ascending and the effect of pulse length on the H_C value is clearly observed. As was found in [9, 12, 13], at the quasistatic

measurements, the $H_C(H_{max})$ dependences for nano-ferrihydrite are *S*-shaped. In principle, despite the data spread in Fig. 4, we may conclude that the $H_C(H_{max})$ dependences in the field range of $H_{max} > 80$ kOe have a negative curvature, i.e., tend to saturation, which agrees qualitatively with the results reported in [9, 12, 13]. Hence, the maximum applied field affects strongly the DMH behavior in nanoferri-hydrite.

On the other hand, if we fix the H_{max} value for the data in Fig. 4 and consider the $H_C(\tau_P)$ dependences (cross section at $H_{max} \approx$ const), then we will see that the coercivity obviously increases with decreasing pulse length: $H_C(\tau_P = 4$ ms$) > H_C(\tau_P = 8$ ms$) > H_C(\tau_P = 16$ ms$)$ at $H_{max} \approx$ const. This behavior can be considered to be the manifestation of the effect of dynamic magnetization switching on the coercivity of the investigated samples.

We may point out roughly that under the dynamic magnetization switching, an increase in the H_{max} value leads to an increase in H_C by approximately the same value as the decrease in the pulse length from 16 to 4 ms. For example, according to the data in Fig. 4, an increase in the H_{max} value to ~100 kOe leads to an increase in H_C of up to $1.3-1.5$ kOe at $\tau_P = 16$ ms (taking into account that the H_C value in the quasistatic magnetic measurements is no more than 10^2 Oe). At $H_{max} \sim 120$ kOe, a decrease in τ_P from 16 to 4 ms leads to an additional increase in H_C to $2.4-2.5$ kOe.

4. CONCLUSIONS

Thus, we experimentally investigated the dynamic magnetization switching of antiferromagnetic ferrihydrite nanoparticles of two types, bacterial and chemical. The investigations included pulsed switching in fields up to 130 kOe and pulse lengths from 4 to 16 ms. For the samples of two types, we established the following regularities. In the temperature range where the effects related to the irreversible behavior of the magnetization curve are insignificant in quasistatic magnetic fields, the hysteresis effects are observed upon pulsed magnetization switching. The coercivity depends on both parameters determining the external field variation rate, i.e., pulse length and maximum applied field. The first factor is unambiguously related to the relaxation processes characteristic of ferromagnetic nanoparticles: a decrease in the pulse length is equivalent to an increase in the frequency or field variation rate, which results in the coercivity growth. However, the observed increase in the coercivity with increasing maximum applied temperature (up to ~10^5 Oe) can be considered to be a feature in the behavior of not only ferrihydrite nanoparticles, but also nanoparticles with an antiferromagnetic order and an uncompensated magnetic moment. According to our data, the similar conclusion can be drawn for

antiferromagnetic nickel oxide nanoparticles. This feature should be taken into account when building a theory of the dynamic magnetic hysteresis of antiferromagnetic nanoparticles. In addition, note that a substantial broadening of the temperature range of existence of the magnetic hysteresis in pulsed fields can become a basis for a wider use of materials based on antiferromagnetic nanoparticles.

REFERENCES

1. S. Mørup, D. E. Madsen, C. Fradsen, C. R. H. Bahl, and M. F. Hansen, J. Phys.: Condens. Matter **19**, 213202 (2007).
2. Yu. L. Raikher and V. I. Stepanov, J. Exp. Theor. Phys. **107**, 435 (2008).
3. Yu. L. Raikher and V. I. Stepanov, J. Phys.: Condens. Matter **20**, 204120 (2008).
4. Q. A. Pankhurst, N. T. K. Thanh, S. K. Jones, and J. Dobson, J. Phys. D **42**, 224001 (2009).
5. K. Dobretsov, S. Stolyar, and A. Lopatin, Acta Otorhinolaryngol. Ital. **35**, 97 (2015).
6. S. A. Makhlouf, F. T. Parker, F. E. Spada, and A. E. Berkowitz, J. Appl. Phys. **81**, 5561 (1997).
7. S. A. Makhlouf, H. Al-Attar, and R. H. Kodama, Solid State Commun. **145**, 1 (2008).
8. C. Diaz-Guerra, M. Vila, and J. Piqueras, Appl. Phys. Lett. **96**, 193105 (2010).
9. N. J. O. Silva, V. S. Amaral, A. Urtizberea, R. Bustamante, A. Millán, F. Palacio, E. Kampert, U. Zeitler, S. de Brion, O. Iglesias, and A. Labarta, Phys. Rev. B **84**, 104427 (2011).
10. J. F. K. Cooper, A. Ionescu, R. M. Langford, K. R. A. Ziebeck, C. H. W. Barnes, R. Gruar, C. Tighe, J. A. Darr, N. T. K. Thanh, and B. Ouladdiaf, J. Appl. Phys. **114**, 083906 (2013).
11. A. E. Bianchi, S. J. Stewart, R. D. Zysler, and G. Punte, J. Appl. Phys. **112**, 083904 (2012).
12. D. A. Balaev, A. A. Krasikov, A. A. Dubrovskiy, S. V. Semenov, S. I. Popkov, S. V. Stolyar, R. S. Iskhakov, V. P. Ladygina, and R. N. Yaroslavtsev, Phys. Solid State **58**, 287 (2016).
13. D. A. Balaev, A. A. Krasikov, A. A. Dubrovskiy, S. I. Popkov, S. V. Stolyar, R. S. Iskhakov, V. P. Lady-

gina, and R. N. Yaroslavtsev, J. Appl. Phys. **120**, 183903 (2016).

14. N. J. O. Silva, V. S. Amaral, and L. D. Carlos, Phys. Rev. B **71**, 184408 (2005).

15. S. A. Makhlouf, F. T. Parker, and A. E. Berkowitz, Phys. Rev. B **55**, R14717 (1997).

16. C. Gilles, P. Bonville, H. Rakoto, J. M. Broto, K. K. W. Wong, and S. Mann, J. Magn. Magn. Mater. **241**, 430 (2002).

17. N. J. O. Silva, A. Millan, F. Palacio, E. Kampert, U. Zeitler, and V. S. Amaral, Phys. Rev. B **79**, 104405 (2009).

18. Yu. L. Raikher, V. I. Stepanov, S. V. Stolyar, V. P. Ladygina, D. A. Balaev, L. A. Ishchenko, and M. Balashov, Phys. Solid State **52**, 298 (2010).

19. Ch. Rani and S. D. Tiwari, Phys. B (Amsterdam, Neth.) **513**, 58 (2017).

20. D. A. Balaev, S. I. Popkov, A. A. Krasikov, A. D. Balaev, A. A. Dubrovskiy, S. V. Stolyar, R. N. Yaroslavtsev, V. P. Ladygina, and R. S. Iskhakov, Phys. Solid State **59**, 1940 (2017).

21. D. A. Balaev, A. A. Dubrovskiy, A. A. Krasikov, S. I. Popkov, A. D. Balaev, K. A. Shaikhutdinov, V. L. Kirillov, and O. N. Mart'yanov, Phys. Solid State **59**, 1547 (2017).

22. I. S. Poperechny, Yu. L. Raikher, and V. I. Stepanov, Phys. Rev. B **82**, 174423 (2010).

23. I. S. Poperechny and Yu. L. Raikher, Phys. B (Amsterdam, Neth.) **435**, 58 (2014).

24. Yu. P. Kalmykov, B. Ouari, and S. V. Titov, J. Appl. Phys. **120**, 053901 (2016).

25. R. H. Kodama and A. E. Berkowitz, Phys. Rev. B **59**, 6321 (1999).

26. D. A. Balaev, A. A. Krasikov, A. A. Dubrovskii, S. V. Semenov, O. A. Bayukov, S. V. Stolyar, R. S. Iskhakov, V. P. Ladygina, and L. A. Ishchenko, J. Exp. Theor. Phys. **119**, 479 (2014).

27. D. A. Balaev, I. S. Poperechny, A. A. Krasikov, K. A. Shaikhutdinov, A. A. Dubrovskiy, S. I. Popkov, A. D. Balaev, S. S. Yakushkin, G. A. Bukhtiyarova, O. N. Mar-

tyanov, and Yu. L. Raikher, J. Appl. Phys. **117**, 063908 (2015).

28. J. G. E. Harris, J. E. Grimaldi, D. D. Awschalom, A. Chiolero, and D. Loss, Phys. Rev. B **60**, 3453 (1999).

29. Chandni Rani and S. D. Tiwari, J. Magn. Magn. Mater. **385**, 272 (2015).

30. M. S. Seehra, V. S. Babu, A. Manivannan, and J. W. Lynn, Phys. Rev. B **61**, 3513 (2000).

31. D. A. Balaev, A. A. Krasikov, A. A. Dubrovskiy, S. I. Popkov, S. V. Stolyar, O. A. Bayukov, R. S. Iskhakov, V. P. Ladygina, and R. N. Yaroslavtsev, J. Magn. Magn. Mater. **410**, 71 (2016).

32. S. V. Stolyar, O. A. Bayukov, Yu. L. Gurevich, V. P. Ladygina, R. S. Iskhakov, and P. P. Pustoshilov, Inorg. Mater. **43**, 638 (2007).

33. S. V. Stolyar, R. N. Yaroslavtsev, R. S. Iskhakov, O. A. Bayukov, D. A. Balaev, A. A. Dubrovskii, A. A. Krasikov, V. P. Ladygina, A. M. Vorotynov, and M. N. Volochaev, Phys. Solid State **59**, 555 (2017).

34. D. A. Velikanov, Vestn. SibGAU, No. 2 (48), 176 (2013).

35. D. A. Balaev, A. A. Krasikov, S. V. Stolyar, R. S. Iskhakov, V. P. Ladygina, R. N. Yaroslavtsev, O. A. Bayukov, A. M. Vorotynov, M. N. Volochaev, and A. A. Dubrovskii, Phys. Solid State **58**, 1782 (2016).

36. S. V. Stolyar, D. A. Balaev, A. A. Krasikov, A. A. Dubrovskiy, R. N. Yaroslavtsev, O. A. Bayukov, M. N. Volochaev, and R. S. Iskhakov, J. Supercond. Nov. Magn. (2017). doi 10.1007/s10948-017-4263-6

37. M. Gich, A. Roig, C. Frontera, E. Molins, J. Sort, M. Popovici, G. Chouteau, D. Martın, Y. Marero, and J. Nogués, J. Appl. Phys. **98**, 044307 (2005).

38. A. A. Dubrovskiy, D. A. Balaev, K. A. Shaykhutdinov, O. A. Bayukov, O. N. Pletnev, S. S. Yakushkin, G. M. Bukhtiyarova, and O. N. Martyanov, J. Appl. Phys. **118**, 213901 (2015).

Translated by E. Bondareva